Article

Inorganic Oxide Core, Polymer Shell Nanocomposite as a High *K* Gate Dielectric for Flexible Electronics Applications

Ashok Maliakal, Howard Katz, Pat M. Cotts, Shekhar Subramoney, and Peter Mirau

J. Am. Chem. Soc., **2005**, 127 (42), 14655-14662• DOI: 10.1021/ja052035a • Publication Date (Web): 30 September 2005

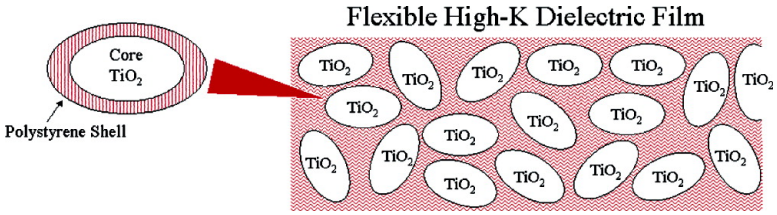

More About This Article

Additional resources and features associated with this article are available within the HTML version:

- Supporting Information
- Links to the 11 articles that cite this article, as of the time of this article download
- Access to high resolution figures
- Links to articles and content related to this article
- Copyright permission to reproduce figures and/or text from this article

View the Full Text HTML

J|A|C|S
ARTICLES
Published on Web 09/30/2005

Inorganic Oxide Core, Polymer Shell Nanocomposite as a High *K* Gate Dielectric for Flexible Electronics Applications

Ashok Maliakal,*,† Howard Katz,† Pat M. Cotts,‡ Shekhar Subramoney,‡ and Peter Mirau§

Contribution from the Department of Materials Research, Bell Laboratories, Lucent Technologies, Murray Hill, New Jersey 07974, DuPont Central Research, Wilmington, Delaware 19880, and Air Force Research Labs, Wright Patterson Air Force Base, Ohio 45433

Received March 30, 2005; E-mail: maliakal@lucent.com

Abstract: Organic/inorganic core shell nanoparticles have been synthesized using high *K* TiO_2 as the core nanoparticle, and polystyrene as the shell. This material is easy to process and forms transparent continuous thin films, which exhibit a dielectric constant enhancement of over 3 times that of bulk polystyrene. This new dielectric material has been incorporated into capacitors and thin film transistors (TFTs). Mobilities approaching 0.2 $cm^2/V{\cdot}s$ have been measured for pentacene TFTs incorporating the new TiO_2 polystyrene nanostructured gate dielectric, indicating good surface properties for pentacene film growth. This novel strategy for generating high *K* flexible gate dielectrics will be of value in improving organic and flexible electronic device performance.

Introduction

Organic materials have received great interest as a new approach to low cost, large area flexible electronics.[1−4] Intense efforts have focused on improving mobility in organic semiconductors.[4] An alternative route to improving device performance is through increasing the dielectric constant of the gate dielectric material while maintaining desirable properties such as flexibility and printability. A higher capacitance dielectric would permit greater charge injection into the semiconductor layer of a thin film transistor for a given gate voltage, thereby permitting the device to operate at lower voltage.[5] Most high *K* ceramic dielectric materials such as titanium dioxide ($K = 31$, anatase; $K = \sim 114$, rutile phase)[6] or strontium titanate ($K \approx 150$)[7] are not easy to process.[8] Easily processible polymers typically have low dielectric constants (i.e., polystyrene ($K = 2.6$) or poly(methyl methacrylate) ($K = 3.12$)).[9,10] Approaches such as loading polymer dielectrics with high capacitance nanoparticles,[11−13] synthesizing nanocrystalline particles inside a bulk polymer matrix,[14] inorganic dielectrics,[15] and very thin films have been attempted.[16,17] Although these methods have produced high capacitance films, they suffer from a lack of flexibility, lack of processibility, or the materials are not likely to respond well to mechanical or thermal stress.

A flexible and printable high *K* dielectric is needed. We report the design, synthesis, and incorporation into devices of a new high *K* flexible gate dielectric material using a core−shell nanoparticle architecture with titanium dioxide as the high capacitance core, and polystyrene as the shell, which we refer to as TiO_2−PS. The core shell nanoparticle structure creates a material, which is in effect pseudo-homogeneous, allowing for smooth film formation and preventing undesirable aggregation and phase separation problems. Silica-polymer core−shell nanoparticles have been synthesized using surface initiated polymerization (SIP).[18,19] However, silica has a relatively low dielectric constant (3.8).[20] Efforts in our lab at SIP from the surface of titanium dioxide nanoparticles have been thwarted by aggregation of initiator coated TiO_2 nanoparticles, prompting us to utilize a grafting method instead. Interestingly, polystyrene-

† Lucent Technologies.
‡ DuPont Central Research.
§ Wright Patterson Air Force Base.

(1) Forrest, S. R. *Nature* **2004**, *428*, 911.
(2) Katz, H. *Chem. Mater.* **2004**, *16*, 4748.
(3) *Printed Organic and Molecular Electronics*; Gamota, D., Brazis, P., Kalyanasundaram, K., Zhang, J., Eds.; Kluwer Academic Publishers: Boston, 2004.
(4) Dimitrakopoulos, C.; Malenfant, P. *Adv. Mater.* **2002**, *14*, 99.
(5) Wallace, R.; Wilk, G. *MRS Bull.* **2002**, *March 2002*, 192.
(6) Roberts, S. *Phys. Rev.* **1949**, *76*, 1215.
(7) Campbell, S.; Kim, H.; Gilmer, D.; He, B.; Ma, T.; Gladfelter, W. *IBM J. Res. Dev.* **1999**, *43*, 383.
(8) Goh, G.; Donthu, S.; Pallathadka, P. *Chem. Mater.* **2004**, *16*, 2857.
(9) Rudd, J. Physical Constants of Poly(styrene). In *Polymer Handbook*, 3rd ed.; Brandrup, J., Immergut, E., Eds.; John Wiley & Sons: New York, 1989; p V81.
(10) Wunderlich, W. Physical Constants of Poly(methyl methacrylate). In *Polymer Handbook*, 3rd ed.; Brandrup, J., Immergut, E., Eds.; John Wiley & Sons: New York, 1989; p V77.
(11) Schroeder, R.; Majewski, L.; Grell, M. *Adv. Mater.* **2005**, *17*, 1535.
(12) Bai, Y.; Cheng, Z.; Bharti, V.; Xu, H.; Zhang, Q. *Appl. Phys. Lett.* **2000**, *76*, 3804.
(13) Su, W.; Lee, J.; Chen, M.; Ho, R. *J. Mater. Res.* **2004**, *19*, 2343.
(14) Yogo, T.; Yamamoto, T.; Sakamoto, W.; Hirano, S. *J. Mater. Res.* **2004**, *19*, 3290.
(15) Aoki, Y.; Kunitake, T. *Adv. Mater.* **2004**, *16*, 118.
(16) Halik, M.; Klauk, H.; Zschieschang, U. *Nature* **2004**, *431*, 963.
(17) Rutenberg, I.; Scherman, O.; Grubbs, R.; Jiang, W.; Garfunkel, E.; Bao, Z. *J. Am. Chem. Soc.* **2004**, *126*, 4062.
(18) Pyun, J.; Matyjaszewski, K.; Kowalewski, T.; Savin, D.; Patterson, G.; Kickelbick, G.; Huesing, N. *J. Am. Chem. Soc.* **2001**, *123*, 9445.
(19) Pyun, J.; Jia, S. J.; Kowalewski, T.; Patterson, G. D.; Matyjaszewski, K. *Macromolecules* **2003**, *36*, 5094.
(20) Ohring, M. *Engineering Materials Science*; Academic Press: San Diego, 1995.

titanium dioxide composites have been investigated previously.[21] In these composites, titanium dioxide and polystyrene were mechanically mixed on a macroscale, and large particle size and aggregation effects as well as poor mixing resulted in a nonhomogeneous system with problems of porosity (air pockets) in the composite material. This previous study on polystyrene−titania illustrates the problem of mixing ceramic and polymeric materials and motivates the need for controlling structure at the nanoscale in high *K* pseudohomogeneous materials such as TiO_2−PS.

Experimental Section

Synthesis and Analysis of Oleic Acid Stabilized Titanium Oxide Nanoparticles (TiO_2−OLEIC). The synthesis of oleic acid stabilized titanium oxide nanoparticles was modified from a literature synthesis.[22] Oleic acid (390 mL, Aldrich tech grade) was dried by heating to 120 °C for 1 h under vigorous nitrogen bubbling, and then allowed to cool to 100 °C. Titanium(IV) isopropoxide (14.76 mL, 50 mmol Aldrich 99.999%) was added. An aqueous solution of trimethylamine-*N*-oxide (TMAO) was made using 11.1 g of TMAO and 50 mL of water. This solution was rapidly added to the heated titanium(IV) isopropoxide/oleic acid. The subsequent mixture was heated for 6 h. After this time, the solution was allowed to cool to room temperature and poured into 1 L of methanol. A fine white precipitate settled from solution. The supernatant was decanted. The wet slurry was washed several times with methanol (an additional 1 L of methanol was used for washing). After most of the supernatant was decanted, the remaining wet slurry was centrifuged to remove most of the remainder of the methanol. The subsequent white solid was dried in the vacuum oven. Approximately 6 g of TiO_2−OLEIC nanoparticles was recovered as a white powder. XRD (vide infra) confirmed that nanoparticles were anatase phase. Elemental analysis of TiO_2−OLEIC (performed by Huffman Laboratories, Golden, CO): %Ti = 38.1, %C = 21.19, %H = 3.81. % weight TiO_2 based on Ti analysis = 63.6%.

Synthesis of 11-Bromo-undecyl-bromo-isobutyrate 5. In an ice bath, bromo-isobutyryl bromide **3** (27.2 g; 126 mmol; Aldrich) was added to 11-bromo-undecanol **4** (26.25 g; 105 mmol; Aldrich) in a solution of triethylamine (10.5 g, 105 mmol) and dichloromethane (400 mL). The solution was allowed to warm to room temperature overnight. After 16 h, the solution was washed several times with dilute hydrochloric acid, then collected and dried on the rotovap. The dark black oil recovered was filtered through a silica gel plug with dichloromethane and concentrated by rotary evaporation. The subsequent clear oil was consistent with 11-bromo-undecyl-bromo-isobutyrate by ^{1}H and ^{13}C NMR. It was used without any further purification in the subsequent synthesis of **5**. ^{1}H NMR ($CDCl_3$): δ 4.14 (2H, t, J = 6.6 Hz), 3.38 (2H, t, J = 7.0 Hz), 1.91 (6H, s), 1.83 (2H, m), 1.66 (2H, m), 1.16−1.47 (14H, m) ppm. ^{13}C NMR ($CDCl_3$): δ 171.6, 66.0, 55.9, 33.9, 32.8, 30.8, 29.3, 29.1, 28.7, 28.3, 28.1, 25.7 ppm.

Synthesis of Initiator 1. Compound **5** (10 g; 25 mmol) and triethyl phosphite (10.8 mL; 62.6 mmol) were combined and heated at 150 °C for 16 h under nitrogen atmosphere. The excess triethyl phosphite was removed under high vacuum. The remaining viscous liquid was run through a silica gel column with dichloromethane to recover **1**, which was clean as determined by NMR. ^{1}H NMR ($CDCl_3$): δ 3.95−4.16 (6H, m), 1.86 (6H, s), 1.49−1.73 (6H, m), 1.13−1.38 (20H, m) ppm. ^{13}C NMR ($CDCl_3$): δ 171.6, 66.0, 61.3 (d, J = 5.5 Hz), 55.9, 30.7, 30.5, 30.4, 29.3, 29.2, 29.0 (d, J = 4.1 Hz), 28.2, 26.3, 25.7, 24.8, 22.3 (d, J = 4.1 Hz), 16.4 (d, J = 5.5 Hz) ppm. ^{31}P NMR ($CDCl_3$): δ 33.9 ppm. Elemental analysis (performed by Robertson Microlit, Madison, NJ). Anal. Calcd for $C_{19}H_{38}O_5BrP$: C, 49.89; H, 8.31; P, 6.78; Br, 17.48. Found: C, 49.91; H, 8.55; P, 6.62; Br, 16.90.

Conversion of 1 to Phosphonic Acid 6.[23] 2.2 mmol of phosphonate **1** and 6.6 mmol of trimethylsilyl bromide (TMSBr) were combined. The reaction was stirred at room temperature for 2 h 45 min, after which volatiles were removed by rotary evaporation. Dioxane (2 mL), water (2 mL), and 6.6 mmol of triethylamine (0.91 mL) were added. After rotary evaporation, the remaining oil was collected. Diethyl ether was added to precipitate a solid, which by NMR was shown to be triethylamine hydrochloride. The collected ether phase was washed with HCl. The aqueous HCl phase was back extracted two times. Collected organics were dried with magnesium sulfate and concentrated by rotary evaporation. After solvent was removed by vacuum pump, a light yellow white solid was recovered in ~40% yield. ^{1}H NMR ($CDCl_3$): δ 8.14 (2H, broad), 4.18 (2H, t, J = 6.6 Hz), 1.95 (6H, s), 1.51−1.90 (4H, m), 1.2−1.5 (16H, m) ppm. ^{13}C NMR ($CDCl_3$): δ 171.7, 66.1, 55.9, 30.8, 30.5, 30.3, 29.4, 29.3, 29.2, 29.1, 29.0, 28.3, 25.7, 22.0. ^{31}P NMR ($CDCl_3$): δ 39.6 ppm. Elemental analysis (performed by Robertson Microlit, Madison, NJ). Anal. Calcd for $C_{15}H_{30}O_5BrP$: C, 44.89; H, 7.48; P, 7.73; Br, 19.93. Found: C, 45.64; H, 7.82; P, 7.65; Br, 19.66.

Synthesis of Phosphonate Terminated Polystyrene 2 through ATRP. Styrene (Aldrich) was passed through an alumina filled column to remove inhibitor. Styrene (10 mL), toluene (Aldrich, 10 mL), **1** (400 mg, 0.87 mmol), and pentamethyldiethylenetriamine (PMDETA; 187 μL; 0.87 mmol) were combined in a two-neck round-bottom flask and degassed for 30 min with nitrogen bubbling. Copper I bromide (125 mg; 0.87 mmol) was added, and the resulting solution was degassed a further 15 min. The entire reaction mixture was then submerged in a 90 °C oil bath and heated at this temperature for 20 h. After this time period, the resulting viscous solution was poured into methanol to precipitate the polystyrene **2**. Polystyrene **2** was recovered after filtering and redissolved into THF followed by precipitation into methanol. This washing procedure was repeated three times. To ensure complete removal of copper salts, solution was taken into THF again and washed with aqueous brine in a separatory funnel several times. After this, the THF solution of **2** was poured into methanol to recover **2** after drying as a white solid. ^{31}P NMR: δ 34.0 ppm.

Ligand Exchange Reaction To Produce Polystyrene Coated Titanium Oxide Nanoparticles (TiO_2−PS). TiO_2−OLEIC (500 mg; with 6.3×10^{-4} mol of surface OH groups/gram based on R = 13.4 nm, assumption of spherical particles, and 24 Å^2 per OH surface group)[24] was mixed with polystyrene **2**, 200 mg (0.074 equivalents per surface OH group), in a dispersion in chlorobenzene. The solution was heated at 100 °C for 24 h. Elemental analysis (performed by Huffman Laboratories, Golden, CO). %Ti = 27.0, %C = 43.39, %H = 4.76, %P = 0.22. Weight% TiO_2 by Ti elemental = 45%. Volume fraction (%volume of TiO_2/total volume) (f): density of TiO_2 = 3.84 g/cm^3. Density of polystyrene = 1.047 g/cm^3. f = (weight fraction TiO_2/density of TiO_2)/[(weight fraction TiO_2/density of TiO_2) + (weight fraction of polystyrene/density of polystyrene)] = 0.182.

Size Exclusion Chromatography with Dynamic Light Scattering. The phosphonate terminated polystyrene **2** was analyzed using size exclusion chromatography coupled with multi-angle static and dynamic light scattering and differential viscometry (SEC/MALS/QELS/Visc). Instrumentation was a Waters 2690 liquid chromatograph, and columns were 2 Polymer Laboratories PLGel Mixed C; analysis was done in tetrahydrofuran (THF). The light scattering instrumentation was a Wyatt Dawn EOS with a QELS (quasielastic light scattering). Data were acquired using the Astra software with the QELS option; correlation functions were acquired for 2 s per slice. The fiber optic for the QELS was positioned at detector #4 (31.4° scattering angle). The concentration eluting at the peak was 3.5 mg/mL.

Dynamic Light Scattering. The particle size and distribution of the nanoparticles were determined using dynamic light scattering.

(21) Khastgir, D.; Maiti, H.; Bandyopadhay, P. *Mater. Sci. Eng.* **1988**, *100*, 245.
(22) Cozzoli, P. D.; Kornowski, A.; Weller, H. *J. Am. Chem. Soc.* **2003**, *125*, 14539.
(23) Freeman, S.; Irwin, W.; Schwalbe, C. *J. Chem. Soc., Perkin Trans. 2* **1991**, 263.
(24) Guerrero, G.; Mutin, P.; Vioux, A. *Chem. Mater.* **2001**, *13*, 4367.

Scheme 1. Synthesis of Phosphonate Terminated Polystyrene (**2**) and Ligand Exchange Reaction of Diethyl Phosphonate Terminated Polystyrene **2** with Oleic Acid Terminated Titanium Oxide To Generate Polystyrene Coated Titanium Dioxide (TiO_2−PS) (PMDETA = Pentamethyldiethylenetriamine)

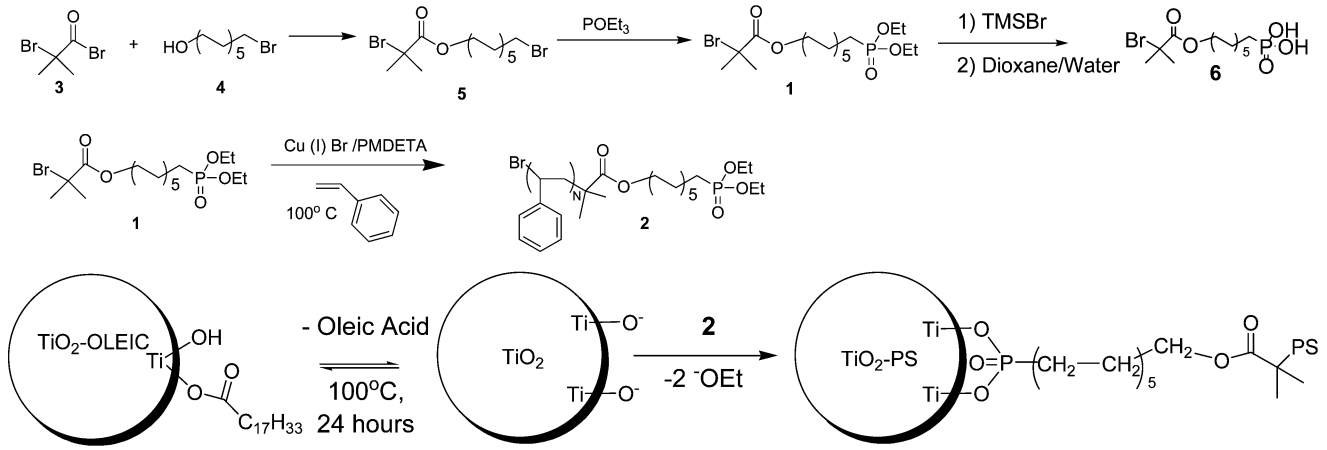

Instrumentation was a Brookhaven instruments BI200SM goniometer. The incident light was 532 nm from a solid-state CW diode-pumped Nd:YAG laser with 50 mW power. Correlation functions and data were acquired using software from Brookhaven instruments. Suspensions in chlorobenzene (10 mg/mL) were analyzed at a scattering angle of 60°. Both angular and concentration dependence were minimal, as expected for dense particles.

Transmission Electron Microscopy (TEM). A drop of a dilute $CHCl_3$-dispersion of nanoparticles was placed on a holey-carbon coated copper TEM grid (200 mesh/3 mm in diameter) and allowed to air-dry. This grid was loaded onto a Philips CM-20 Ultratwin high-resolution TEM, which was operated at an accelerating voltage of 200 kV for obtaining the high-resolution images. Elemental verification of the TiO_2 was done by a Link energy dispersive spectroscopy system mounted on the Philips CM-20 column.

FT-IR. FT-IR was performed using a Nicolet Magna-IR 560. Samples were prepared in a KBR pellet.

Solid-State NMR. Solid-state carbon and phosphorus NMR spectra were acquired at 100 and 162 MHz on a Varian 400 Unity NMR spectrometer using cross polarization and magic-angle sample spinning in a 7.5 mm Chemagnetics probe. The carbon, phosphorus, and proton field strengths were 50 kHz for cross polarization and decoupling, and the cross polarization time was 1 ms. The spectra were referenced to the methyl carbon of hexamethylbenzene at 17.35 ppm for the carbon spectra and to 85% phosphoric acid at 0 ppm for the phosphorus spectra.

Device Preparation and Measurements. Top contact geometry was used in the transistor devices. ITO-glass was used as the substrate. Films were deposited from solution of TiO_2−PS/chlorobenzene (10−20 wt %/volume) using a Headway Research spin coater, at spin speeds of 1000 rpm for 45 s. For capacitors, gold top contacts were evaporated (0.0855 mm^2 area circles, and 100 nm thick) using a shadow mask at a rate of ∼0.1 nm/s. For TFTs, pentacene was evaporated at ∼0.3−0.4 Å/s (film thickness 50 nm), followed by gold top contacts (bars, width 3 mm, channel length 0.32 mm, W/L = 9.4, 100 nm thick). All evaporations were performed using an Edwards Auto 306 Vacuum Coater. Thin film characterization was performed using a probe station and HP 4155A Semiconductor Parameter Analyzer. Capacitance measurements were made on an HP 4284A LCR meter.

Results and Discussion

Synthesis. Titanium oxide nanoparticles were synthesized by hydrolysis of titanium IV isopropoxide in the presence of aqueous trimethylamine *N*-oxide (TMAO) and oleic acid based on a literature procedure.[22] This synthesis provided oleic acid stabilized titanium oxide nanoparticles (TiO_2−OLEIC), which are cylindrical in shape (see TEM data; vide infra). These particles disperse well in chlorobenzene and form transparent dispersions. XRD confirms these nanoparticles to be crystalline and anatase phase (see Figure 3).[22]

Atom transfer radical polymerization (ATRP)[25] was used to synthesize narrowly disperse (PD < 1.1) phosphonate terminated polystyrene. Compound **1**, which contains the α-bromo-ester ATRP initiating functionality, was synthesized as described in Scheme 1. The initiator was designed with a phosphonate moiety because phosphonates are known to bind strongly to titanium oxide surfaces.[24,26,27] Initiator **1** was used to polymerize styrene using copper I bromide/pentamethyldiethylenetriamine catalyst[28] to generate diethyl phosphonate terminated polystyrene **2**. Polymer **2** was found to have M_w = 8400 and polydispersity 1.05 by GPC.

Polymer **2** was used in a ligand exchange reaction with TiO_2−OLEIC to generate TiO_2−PS (see Scheme 1). The ligand exchange reaction proceeds because the oleic acid binds reversibly to the titanium dioxide surface and can be displaced by the phosphonate group,[22] which forms a stronger bond to the titanium dioxide surface (see Scheme 1).[24] 0.074 equiv of **2** is used per surface −OH on TiO_2 (concentration of surface −OH sites on TiO_2 calculated on the basis of mean particle size and surface area, and the area per surface −OH for TiO_2, which is reported in the literature to be 24 $Å^2$ per OH surface group).[24] A less than stoichiometric concentration was used to maintain a high volume fraction of high *K* titanium dioxide. For this reason, not all oleic acid is removed during the ligand exchange as can be observed in SS-NMR and FT-IR (see Supporting Information).

Characterization of Phosphonate Binding to TiO_2. Solution and solid-state NMR as well as FT-IR were applied to the characterization of the binding between the PS−PO_3Et_2 **2** and the titanium oxide surface.

The ^{31}P chemical shifts for the phosphonic acid **6** (see Scheme 1) and the diethyl phosphonate **1** are 39.6 and 34.5 ppm, respectively, which are consistent with literature for alkyl substituted phosphonate esters[29] and phosphonic acids.[26] In

(25) Matyjaszewski, K.; Xia, J. *Chem. Rev.* **2001**, *101*, 2921.
(26) Gao, W.; Dickinson, L.; Grozinger, C.; Morin, F.; Reven, L. *Langmuir* **1996**, *12*, 6429.
(27) Mitchell, M.; Sheinker, V.; Mintz, E. *J. Phys. Chem. B* **1997**, *101*, 11192.
(28) Xia, J.; Matyjaszewski, K. *Macromolecules* **1997**, *30*, 7697.
(29) Gorenstein, D. *Phosphorus-31 NMR: principles and applications*; Academic Press: Orlando, FL, 1984.

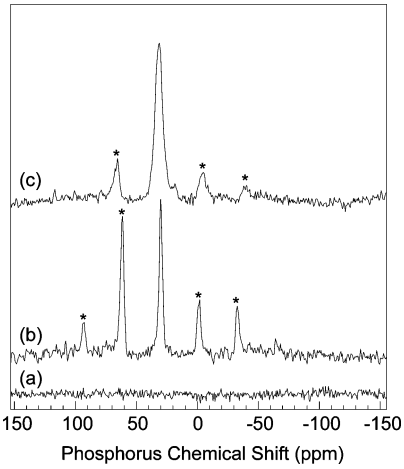

Figure 1. The 162 MHz solid-state phosphorus NMR spectra for (a) TiO_2-OLEIC, (b) $PS-PO_3Et_2$, and (c) $PS-TiO_2$. The spectra were acquired at 162 MHz using magic-angle sample spinning and cross polarization with a 1 ms contact time. The spinning sidebands are marked (∗). The isotropic peak positions in (b) and (c) are 32.0 and 33.8 ppm (referenced to an external sample of 85% H_3PO_4).

the case of the polystyryl phosphonate **2**, the solution ^{31}P NMR resonance occurs at 34.0 ppm, 0.5 ppm upfield from the analogous small molecule **1**. Solid-state NMR spectra on **2** show a single resonance at 32 ppm (see Figure 1), a 2 ppm upfield shift from the solution spectra. In the case of TiO_2-PS, the phosphorus isotropic chemical shift is now 33.8 ppm. This change in chemical shift is accompanied by a larger line width and a greater degree of asymmetry in the spectra. Also, there is no indication of any free **2** in the solid-state NMR for TiO_2-PS, as there are no sharp lines in the spectra indicative of this species. The data are consistent with previous studies of binding of methyl[30] and octadecyl phosphonic acids[26] to titanium oxide surfaces (i.e., slight downfield shift with respect to the free acid and line broadening). Furthermore, ^1H NMR studies performed on the TiO_2-PS, which is swollen in $CDCl_3$, do not show the ethyl resonance expected from residual ethyl phosphonate ester linkages (see Supporting Information). These data support the conclusion that the ethoxy groups are displaced upon ligand exchange and suggest that the nature of the binding between TiO_2 and the phosphonate is through a tridentate attachment of the phosphonate to the titanium oxide surface. Phosphonate ^{31}P NMR resonances are not expected to change dramatically with substitution of carbon for titanium,[29] and so the ^{31}P NMR is also consistent with a tridentate binding mode as has been previously proposed in the literature.[30] The ^{13}C solid-state NMR spectra for TiO_2-PS show the expected resonances for polystyrene and also show peaks consistent with residual oleic acid (see Supporting Information). The residual oleic acid is expected, because a substoichiometric amount of polystyryl phosphonate (**2**) was used in the ligand exchange reaction.

The FT-IR data illustrated in Figure 2 reveal further information of the nature of the binding between the phosphonate linkage and the titanium oxide surface. Figure 2a shows the P═O stretch at 1247 cm^{-1} and the ester carbonyl stretch at 1726 cm^{-1}, which is consistent with literature.[30,31] Figure 2b shows the IR spectra for TiO_2-PS and TiO_2-oleic acid. The spectra

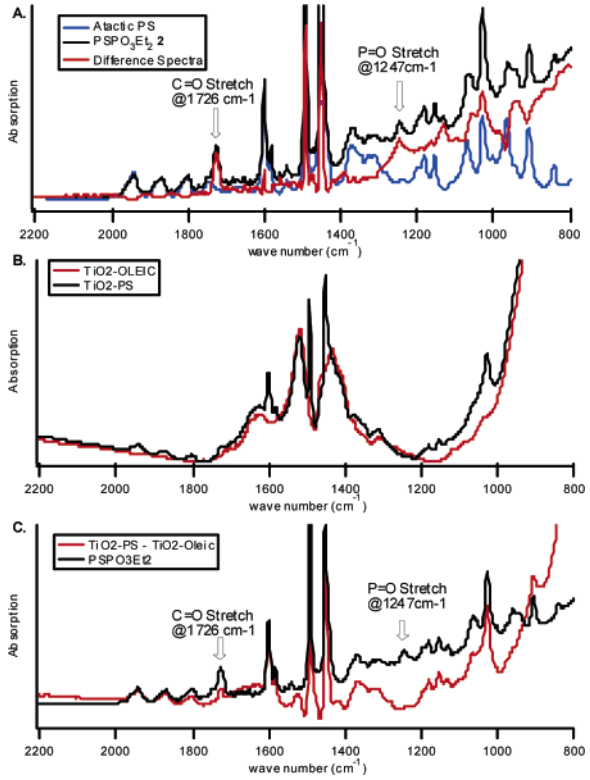

Figure 2. FTIR spectra for (A) **2** as compared to atactic polystyrene, (B) TiO_2-OLEIC and TiO_2-PS, and (C) comparison of TiO_2-PS and **2**.

for TiO_2-PS clearly show the vibrational pattern for the aromatic groups in polystyrene between 1750 and 2000 cm^{-1}. Figure 2c presents the comparison of the starting material $PS-PO_3Et_2$ (**2**) spectrum with the spectrum of TiO_2-PS after subtracting the TiO_2-oleic acid background spectra. In this comparison, we can clearly see that the ester carbonyl stretch at 1728 cm^{-1} is preserved. However, at 1247 cm^{-1}, the P═O is notably absent. The absence of the P═O stretch at 1728 cm^{-1}, in addition to the solid-state NMR data, give strong evidence to the involvement of the P═O in binding to the titanium oxide surface and is consistent with other studies on binding of phosphonates and phosphonic acids to titanium oxide.[24,26,30,32] The detailed nature of the binding of phosphonates to titanium dioxide is still not fully understood.[30] A recent HF-DFT study has calculated that the most stable binding mode of phosphonic acids to titanium dioxide is a monodentate interaction between the P═O oxygen and a surface titanium.[32] Our data are consistent with binding through the phosphonyl oxygen, and possibly also through titanate esters, because the ethoxy groups appear to have been displaced. However, further experimental efforts beyond the scope of this study are required to more definitively characterize the nature of this linker chemistry. FT-IR data, consistent with NMR data, show a broad absorption at 3400 cm^{-1} indicative of residual oleic acid in the TiO_2-PS composite (see Supporting Information). However, no additional carbonyl resonance is observed either in TiO_2-OLEIC or in TiO_2-PS (see Figure 2B), which suggests that all of the oleic acid present is attached through the carbonyl group to the TiO_2 surface.

(30) Falaras, P.; Arabatzis, I.; Stergiopoulos, T.; Papavassiliou, G.; Karagianni, M. *J. Mater. Process. Technol.* **2005**, *161*, 276.
(31) Nakanishi, K.; Solomon, P. *Infrared Absorption Spectroscopy*, 2nd ed.; Holden-Day, Inc.: San Francisco, 1977.
(32) Nilsing, M.; Lunell, S.; Persson, P.; Ojamae, L. *Surf. Sci.* **2005**, *582*, 49.

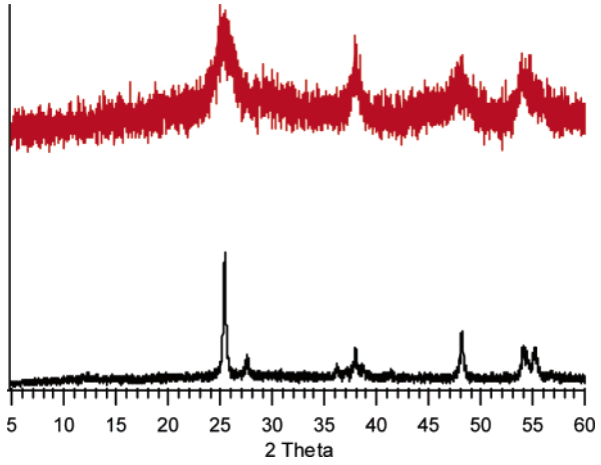

Figure 3. XRD on TiO_2−OLEIC (red) and commercial titanium oxide nanoparticles (anatase phase).

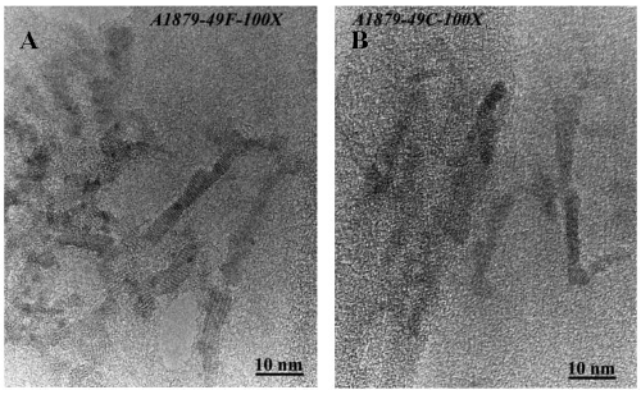

Figure 4. Representative TEM on (A) TiO_2−OLEIC and (B) TiO_2−PS nanoparticles.

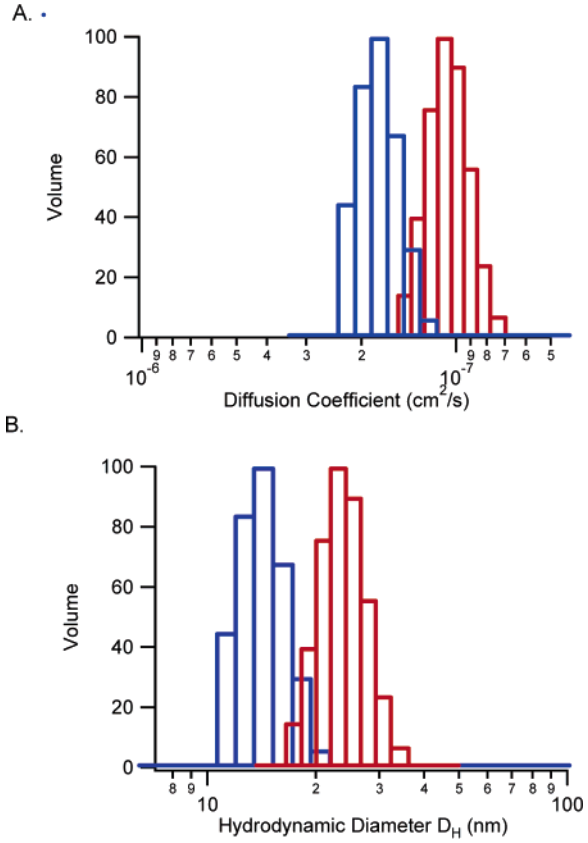

Figure 5. DLS on TiO_2−OLEIC and TiO_2−PS. (A) Diffusion constant data from DLS measurement (see Experimental Section for details). (B) Distribution of diameters for equivalent hydrodynamic spheres calculated from diffusion constant data. Blue histogram is TiO_2−OLEIC nanoparticles. Red histogram is distribution of TiO_2−PS nanoparticles.

Materials Characterization. XRD, TEM, and dynamic light scattering (DLS) studies have been used to characterize the shape, size, and morphology of TiO_2−PS.

XRD data for TiO_2−OLEIC nanoparticles and for commercial anatase phase TiO_2 nanoparticles are illustrated in Figure 3. The peak positions are consistent with anatase phase titanium dioxide. The peak broadening for the TiO_2−OLEIC nanoparticles is due to their small size, which can be estimated using the full width at half max (fwhm) for these peaks and the Scherrer equation.[33] Using this analysis, the effective crystal size is found to be approximately 6 nm.

TEM images of TiO_2−OLEIC and TiO_2−PS are presented in Figure 4. The cores are seen to be cylindrical in shape with an aspect ratio between 4 and 6. Using several different TEM images and averages for approximately 12 clearly resolved titanium dioxide cores, average statistics for the particle core sizes were calculated. In the case of TiO_2−OLEIC, the particles were found to be 18 ± 6 nm in length and 4.1 ± 1 nm wide. The TiO_2−PS samples were found to be 19 ± 5 nm long and 3.4 ± 1 nm wide. Within experimental uncertainty, we conclude that the titanium oxide core size does not change upon functionalization with polystyrene, as we would expect. The differences are likely due to the small sampling size, and the mean values are within experimental uncertainty. The atomic level planes of the titanium oxide cores of individual particles in these images are clearly visible, indicating that the nanoparticles are crystalline, as has been previously demonstrated by XRD data. The particle sizes from TEM can be reconciled with the estimated size from the Scherrer equation because the Scherrer equation yields a value for the average crystal dimension.[33] This average value (6 nm) is in reasonable agreement with the average of the long (18 nm) and two short axes (4.1 nm) for the cylindrical crystals observed by TEM, which is 8.7 nm. TEM cannot image amorphous material such as polystyrene directly. To better assess the shell material as well as to examine the properties of the entire ensemble of particles, dynamic light scattering is used as a complementary method to TEM.

The correlation functions from dynamic light scattering data on TiO_2−OLEIC and TiO_2−PS were fit with the method of cumulants. The measured diffusion coefficients were used to determine the diameters of equivalent hydrodynamic spheres. The distribution of diffusion constants and hydrodynamic diameters for TiO_2−OLEIC and TiO_2−PS are presented in Figure 5. The average diameters for equivalent hydrodynamic spheres for TiO_2−OLEIC and TiO_2−PS are 13 and 23 nm. The distribution of diffusion coefficients is quite narrow for both TiO_2−OLEIC and TiO_2−PS, which is indicative of narrow particle size distributions. However, because TEM data reveal that TiO_2−OLEIC is in fact cylindrical rather than spherical, we have used a prolate ellipsoidal model and the axial ratio of 5 ± 2 from TEM data to assess the length of cylindrical particles

(33) Klug, H.; Alexander, L. *X-ray Diffraction Procedures for Polycrystalline and Amorphous Materials*; John Wiley and Sons: New York, 1954; Chapter 9.

based on our DLS data. Using this model and eq 1, we can estimate the mean length for the ensemble of TiO_2−OLEIC particles:

$$\frac{R_H}{R_S} = \frac{(1-p^2)^{1/2}}{p^{2/3}\ln[1+(1-p^2)^{1/2}/p]} \quad (1)$$

where R_H is the measured hydrodynamic radius from DLS, and R_S is the radius of a sphere of equivalent volume to the ellipsoid of axial ratio p^{-1}. The TiO_2−OLEIC acid particles are found to have a mean length of 16 nm ± 5 nm, which is consistent with the value of 18 ± 6 nm calculated from the TEM data. Upon functionalization with polystyrene, the measured hydrodynamic particle diameter from the DLS nearly doubles from 13 to 23 nm, whereas the TEM images, which resolve only the TiO_2 cores, show little change. However, the particle size distribution from DLS remains monomodal and quite narrow, which is consistent with a clean functionalization of the nanoparticles and no significant aggregation of particles on functionalization. The DLS technique is highly sensitive to the presence of even small amounts of aggregates, which scatter more intensely. Solid-state NMR data and FT-IR data (vide supra) are also consistent with clean functionalization, as it can be observed from these data (see Figures 1 and 2) that complete reaction of the phosphonyl group of **2** with the TiO_2 surface has occurred, indicating that all polystyrene is surface bound. Furthermore, the lack of particle aggregation in the TEM data is consistent with the increase in particle size in the DLS data being due to the polymer shell and not aggregation effects. The thickness of the oleic acid shell of TiO_2−OLEIC is estimated to be approximately 0.5−1 nm, and therefore would be expected to contribute a maximum of ~1−2 nm to the thickness of TiO_2−OLEIC in addition to the core.[34] Because the uncertainty in the particle size is much greater than the oleic acid thickness, and, furthermore, the oleic acid is not completely displaced by the polystyryl phosphonate **2** (0.075 equiv of phosphonate per surface −OH was used), it is not considered in the subsequent analysis.

The hydrodynamic radius R_H of the polystyrene **2** can be measured by GPC with DLS detection (see Figure 6). In this case, R_H for **2** is 2.1 ± 0.1 nm. Assuming that the TiO_2 core particles are unchanged, as can be seen in the TEM, the increase in the hydrodynamic radius from the TiO_2−OLEIC to the TiO_2−PS can be attributed to the attached PS. A monolayer of polystyrene is expected to increase the radius of TiO_2−PS by ~4 nm, and the diameter of TiO_2−PS by ~8 nm.[35] Comparing the D_H values for TiO_2−OLEIC and TiO_2−PS, we see that the change in diameter of ~10 nm upon functionalization with PS is consistent with expectation for the attachment of a layer of PS and supports the conclusion that the polystyrene chains form a shell around the titanium oxide core that is roughly 1 coil thick.

Devices. Capacitors were fabricated using TiO_2−PS as the dielectric. The TiO_2−PS was spun from chlorobenzene solution (10−20% weight/volume) onto indium tin oxide (ITO) on glass, yielding films that ranged in thickness (d) from 0.5 to 1.25 μm. The volume % of titanium dioxide (volume of TiO_2/total volume) in these films was 18.2% as calculated in the Experimental Section. Gold top electrodes (area (A) = 0.085 mm^2) were then evaporated onto these substrates. The capacitance (C) was measured and used to calculate the dielectric constant using eq 2.

$$K = Cd/\epsilon_o A \quad (2)$$

where ϵ_o is the permittivity of space. The dielectric constants at 1 kHz for films of three different thicknesses are presented in Figure 7. For the thinnest film (0.5 μM), the calculated dielectric constant is approximately 15% larger than that for thicker films. The larger dielectric constant in the thinner film could be due to interfacial effects that are more prominent in the thinner films. However, more detailed investigations are required to exclude other possibilities. Capacitors were also made with lower volume fractions of titanium dioxide. The data

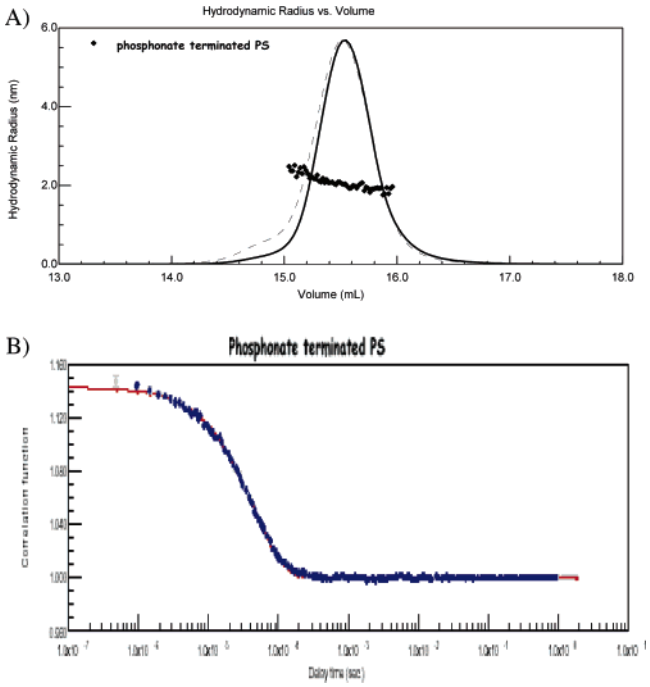

Figure 6. (A) GPC trace for **2**. The points shown are the hydrodynamic radius, R_h, determined at each slice across the distribution for **2**. The solid curve is the refractive index (concentration) chromatogram, and the dashed curve is the light scattering intensity chromatogram at 90° scattering angle. (B) A representative correlation function for the slice at 15.25 mL elution volume, near the peak maximum.

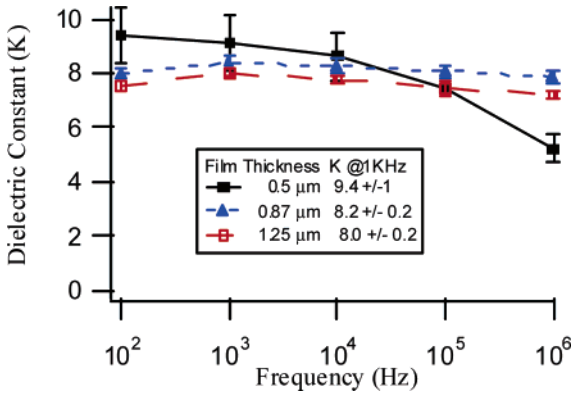

Figure 7. Frequency dependence of K for films of TiO_2−PS (18.2 vol % TiO_2) of varying thickness.

(34) Tadmor, R.; Rosenweig, R.; Frey, J.; Klein, J. *Langmuir* **2000**, *16*, 9117.
(35) Fetters, L.; Hadjichristidis, N.; Lindler, J.; Mays, J. *J. Phys. Chem. Ref. Data* **1994**, *23*, 619.

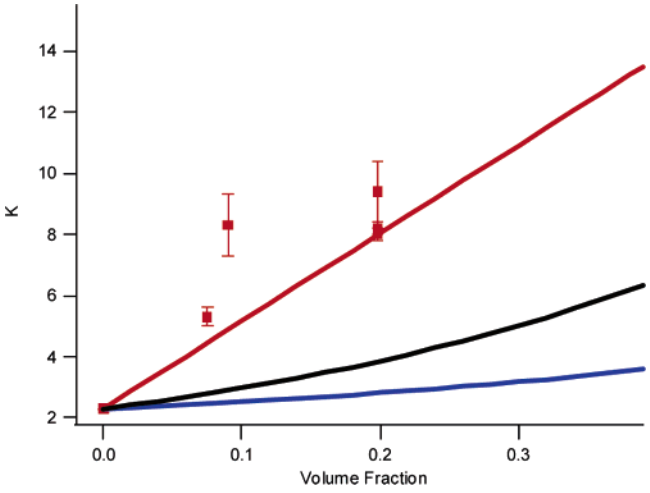

Figure 8. Data for *K* for films (red squares with error bars) as compared to predictions for *K* for composite films using the parallel model (red), the log mixture model (black), and the series model (blue).

from all capacitors measured are presented in Figure 8, along with curves of dielectric constant versus composition for composites of parallel, series geometries as well as a log-mixture model for composite dielectrics.[36] Comparing our data with these models, it is clear that the measured dielectrics fit best with the parallel model, and in some cases have higher *K* values than would be predicted by the parallel model for composite dielectrics. These models are dependent on a value of $K = 31$ for anatase phase titanium dioxide. However, it is not clear whether the dielectric constant of nanoscale titanium dioxide would be the same as that for bulk anatase titanium dioxide. With these sources of uncertainty in mind, the data are at least in qualitative agreement with the parallel model for composite dielectrics.

The frequency dependence of *K* is presented in Figure 7. For the thinnest film investigated, higher dielectric constants are observed at low frequency (100 Hz). However, the frequency-dependent drop in observed dielectric constant is much steeper than for thicker films. Films at 0.87 and 1.25 μm exhibit slightly lower overall dielectric constant, but flatter frequency response. The drop in observed values for *K* with frequency has been observed previously in the macrocomposite of polystyrene and titanium dioxide.[21] The frequency range investigated ($100-10^6$Hz) is the frequency range where orientational polarization effects are operative.[20] This suggests that the drop in *K* with increasing frequency in this case is due to some sort of large scale reorientational motion, which is being frozen out with increasing frequency. Because the effect is only operative on the thinner films, it suggests that the effect may be dependent on the electric field[37] and/or due to an interfacial/surface effect, which is not as important in thicker films; however, other possibilities cannot be excluded without further experimentation beyond the scope of the current study.

Pentacene thin film transistors (TFTs) were fabricated using TiO_2-PS as the gate dielectric (see Figure 9). These TFTs operate at low threshold voltage (-2 V), suggesting a low trap density, and exhibit reasonably high mobilities. This suggests that the structure of our dielectric film is compatible with good

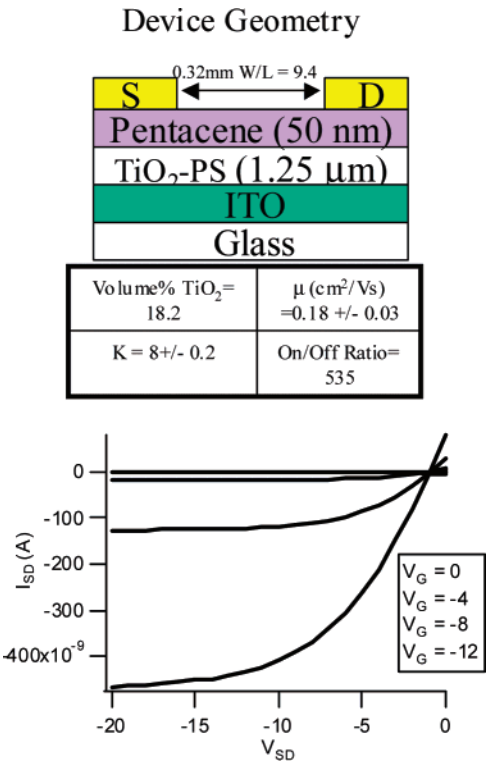

Figure 9. Device geometry and transistor characteristics for pentacene TFT using 20 mol % TiO_2-PS as gate dielectric.

pentacene film growth and adhesion. The average mobility for these devices is 0.18 ± 0.03 cm^2/V·s, which without any further optimization is only approximately an order of magnitude lower than the highest published values for pentacene devices in TFTs.[16,38−40] Further efforts to improve film smoothness and reduce channel length (currently ~300 μm) are expected to increase mobility. The on/off ratio (535) is reasonably high for these unpatterned pentacene devices, indicating low leakage currents through the dielectric. Loss tangents for capacitance measurements are below 0.1. Dielectric breakdown occurs at fields exceeding 2×10^6 V/m.

Conclusions

We have designed and synthesized a novel core−shell-nanoparticle based gate dielectric using titanium oxide as the core material and polystyrene as the flexible shell. The high *K* core lends high capacitance while the flexible shell endows the material with good dispersability and film-forming properties, which are anticipated to make TiO_2-PS easier to print. The chemical linkage between the polymer shell and the titanium oxide surface has been characterized by solid-state NMR and FT-IR. The binding mode is shown to be through the oxygen of the phosphonyl group, and possibly through additional titanate ester linkages. The shape and size distribution of $TiO_2-OLEIC$ and TiO_2-PS were assessed using TEM and DLS. Particles are demonstrated to be cylindrical with an aspect ratio between roughly 4−6. DLS data show a narrow distribution in particles sizes for $TiO_2-OLEIC$, which is preserved upon functional-

(36) Mazur, K. Polymer-Ferroelectric Ceramic Composites. In *Ferroelectric Polymers*; Nalwa, H., Ed.; Marcel Dekker: New York.
(37) Wang, T. *The Applications of Ferroelectric Polymers*; Chapman and Hall: New York, 1988.
(38) Kelley, T.; Boardman, L.; Dunbar, T.; Muyres, D.; Pellerite, M.; Smith, T. *J. Phys. Chem. B* **2003**, *107*, 5877.
(39) Klauk, H.; Halik, M.; Zschieschang, U.; Eder, F.; Schmid, G.; Dehm, C. *Appl. Phys. Lett.* **2003**, *82*, 4175.
(40) Klauk, H.; Halik, M.; Zschieschang, U.; Schmid, G.; Radlik, W.; Weber, W. *J. Appl. Phys.* **2002**, *92*, 5259.

ization with polystyrene. TiO_2−PS was incorporated into capacitors and pentacene thin film transistors. The dielectric constant was measured in capacitors and exhibits up to a 3.6 times enhancement in *K* as compared to polystyrene at only 18.2 volume % loading. Pentacene TFTs exhibit mobilities approaching 0.2 $cm^2/V \cdot s$. Efforts are underway to further enhance the dielectric constant of this material through higher loading fractions and device optimization.

Acknowledgment. We thank Zhiqiang Liu, Geoff Nunes, Theo Siegrist, Ed Chandross, and Andy Lovinger for helpful discussions. In addition, we are grateful to the reviewers for their insightful comments and suggestions, which have been incorporated to improve this manuscript. This work is supported in part by a NIST ATP grant (Cooperative Agreement Number: 70NANB2H3032).

Supporting Information Available: Additional FT-IR and solid-state NMR data. This material is available free of charge via the Internet at http://pubs.acs.org.

JA052035A